# Evaluation of Iron-Aluminide CVD Coatings for High Temperature Corrosion Protection

**B. A. Pint, Y. Zhang†, P. F. Tortorelli, J. A. Haynes and I. G. Wright**
*Metals and Ceramics Division, Oak Ridge National Laboratory, Oak Ridge, TN 37831-6156*
*†Center for Manufacturing Research, Tennessee Technological University, Cookeville, TN 38505-0001*

Chemical vapor deposited (CVD) Fe-Al coatings are being investigated to address fundamental issues concerning aluminide coating performance and lifetime. By using a well-controlled laboratory CVD procedure, the coatings are uniform in composition, purity and microstructure. A typical ferritic steel, Fe-9Cr-1Mo, and an austenitic stainless steel, 304L (nominally Fe-18Cr-9Ni), were coated to examine differences in the two types of substrates. For both substrates, the as-deposited coating consisted of a thin (<5 μm), Al-rich layer above a thicker (30–50 μm), lower Al content layer. To follow-up on initial results, which showed good coating performance in air+10vol.%$H_2O$ and $H_2S$-$H_2O$-$H_2$-Ar, cyclic tests were performed in both environments at 800°C and more detailed characterization of the isothermally exposed coatings was conducted. During 2–5, 25h cycles at 800°C in $H_2S$-$H_2O$-$H_2$-Ar, CVD coatings on both substrates showed progressively more attack during each cycle. However, in 1h cycles at 800°C in air + 10vol.%$H_2O$, the coatings showed excellent performance, similar to cast Fe-(15–20at.%)Al specimens. The uncoated alloys were significantly attacked during all of these tests. Thermal expansion measurements show Al additions up to 20at% have little effect on the mean expansion of ferritic alloys but the higher thermal expansion of austenitic steels may be a better match with $Fe_3Al$ coatings.

## INTRODUCTION

A current interest is to increase the temperature capabilities of ferritic and austenitic alloys for power generation applications. However, these alloys owe their oxidation resistance to the formation of Cr-containing oxides which become less protective at higher temperatures and in steam or exhaust environments [1–2]. Iron aluminides are well-known to have excellent oxidation and sulfidation resistance due to the formation of an external, protective alumina scale [3–7]. An additional benefit of forming an alumina scale, compared to chromia or silica scales, is its resistance to carburization [8] and to vaporization in exhaust environments [9]. Thus, an aluminide coating could improve the oxidation resistance of ferritic and austenitic steels and enable their use at higher temperatures and/or in environments where they may not have adequate oxidation resistance.

In order to gain confidence in the performance of such coatings, more fundamental information is needed on their potential applications and benefits. Of particular interest is their performance in water vapor- and/or sulfur-bearing gases at high temperature and the prediction of coating lifetime as a function of its Al content. Chemical vapor deposited (CVD) Fe-Al coatings [10] are being investigated to provide some of this information. With a well-controlled laboratory CVD procedure, the coatings can be made uniform in composition, purity and microstructure over the entire substrate. One ferritic and one austenitic substrate were selected to examine differences in the two types of substrates. Two issues of particular concern are modeling the effect of time and temperature on the loss of Al from the coating into the substrate and understanding possible compatibility problems between candidate substrates and Fe-Al coatings which can have substantially different coefficients of thermal expansion (CTE) [11–12]. The present work has focused on characterizing as-fabricated coatings and cyclic oxidation and sulfidation experiments. A cyclic test could expose any potential problems with CTE mismatch in the coating system or a problem with protective oxide scale adhesion.

## EXPERIMENTAL PROCEDURE

The substrates used in this study were a ferritic alloy, Fe-9Cr-1Mo, and an austenitic stainless steel, 304L (nominally Fe-18Cr-9Ni). The CVD coating apparatus and method have been described previously.[10] A standard exposure of 6 h at 900°C was used. Because the coatings contain significantly less Al than a typical $Fe_3Al$ alloy such as FAS or FAL (28at.%Al), model Fe-Al alloys containing 15at.%(8wt.%) and 20at.%(11wt.%) were cast for comparison in oxidation tests and CTE measurements. All of the specimens were polished to a

0964-3409/01/01/00035–12
© 2001 Science Reviews

0.3 μm alumina finish either prior to coating or prior to exposure. As a final treatment, all specimens were ultrasonically cleaned in acetone and methanol.

High temperature exposures were conducted at 800°C. The cyclic oxidation testing in air with 10 ± 0.5vol.%$H_2O$ was done in an automated test rig with a cycle consisting of 1h at temperature and 10min cooling at room temperature. Both ends of the vertical reaction tube were closed and the water vapor was controlled in the carrier gas by a water injection system described elsewhere [2]. Cyclic testing in $H_2S$-$H_2O$-$H_2$-Ar ($P_{S_2}$ = $10^{-6}$atm; $P_{O_2}$ = $10^{-22}$atm) was done manually in a Cahn microbalance with a cycle time of approximately 25h and a cooling time of >1 h. Before and after exposure, selected specimens were examined by light microscopy, field emission gun, scanning electron microscopy (SEM) equipped with energy dispersive x-ray analysis (EDXA), x-ray diffraction (XRD), and electron probe microanalysis (EPMA) using wavelength dispersive x-ray analysis. The surface product of cross-sectioned specimens was protected by Cu-plating the specimen prior to mounting in epoxy. Thermal expansion measurements were performed on specimens (3–4 mm diameter, 1cm or 2.5 cm long) of several alloys up to 1300°C on a Theta Industries dual push rod differential dilatometer.

## RESULTS AND DISCUSSION

### *As-Deposited coating Characterization*

Figure 1 shows a cross-section of the as-deposited aluminide coating on Fe-9Cr-1Mo. From the atomic number contrast of the back-scattered electron image, there appears to be a ≈3 μm thick outer layer and a ≈60 μm thick inner layer. Figure 2 shows a composition profile from the outer surface into the substrate. The outer layer contains ≈20at.%Al but a gradual decrease in the Al content was observed back to a depth of ≈50 μm, which is slightly less than expected from the image in Figure 1.

Figure 3 is a EPMA back-scattered electron image of a cross-section of the as-deposited coating on 304L. In this case, the presence of Ni in the substrate results in a more complicated microstructure. The outer layer is slightly thicker than with the ferritic substrate, ≈5 μm. The composition profile in the coating, Figure 4, indicates that this layer is rich in Ni (>20at.%) and contains more Al (≈35at.%) than the outer layer on Fe-9Cr-1Mo. However, the inner layer on 304L is only ≈35 μm thick. This difference is attributed to slower diffusion in the austenitic substrate which also affects its oxidation behavior [13–14]. Again, the inner layer on 304L contains more Al than on Fe-9Cr-1Mo and appears to have a more abrupt change in composition at the interface with the substrate.

The coatings also were characterized by XRD. Figure 5 shows one peak associated with (211) in the α structure or (422) in the $DO_3$ ($Fe_3Al$) structure. For the coatings on both substrates, the two peaks are due to the $K\alpha_1$ and $K\alpha_2$ Cu radiation. For comparison, diffraction data for cast alloys with different Al contents also are plotted. These peaks show a shift with increasing Al content. They do not show a split peak because a faster scan rate was used.

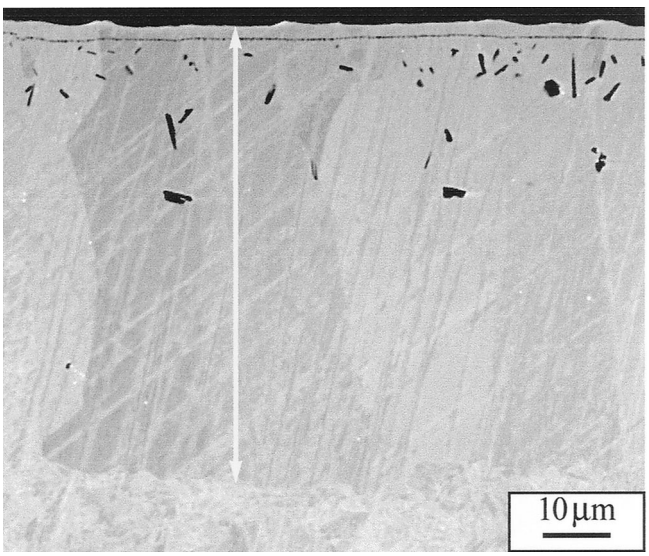


**Figure 1** EPMA back-scattered electron image of the as-deposited aluminide coating on Fe-9Cr-1Mo.

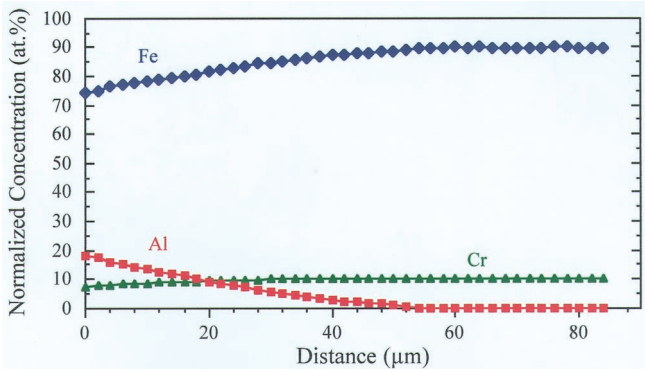


**Figure 2** Fe, Al and Cr profiles in the as-deposited coating on Fe-9Cr-1Mo using EPMA.

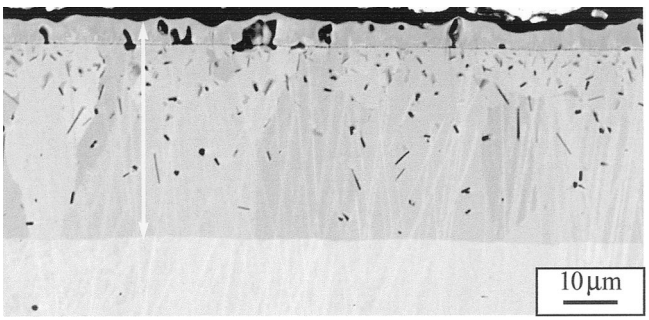


**Figure 3** EPMA back-scattered electron image of the as-deposited aluminide coating on 304L.

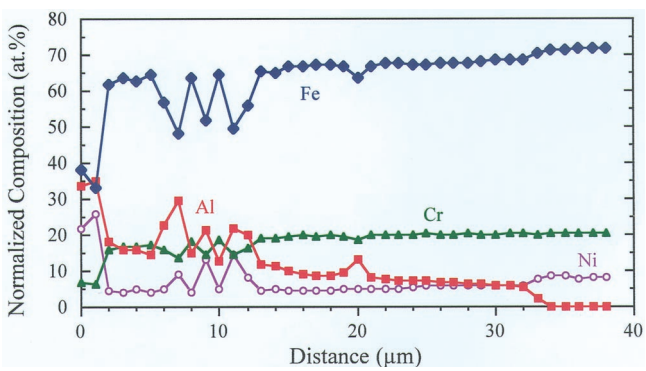


**Figure 4** Fe, Al Cr and Ni profiles in the as-deposited coating on 304L using EPMA.

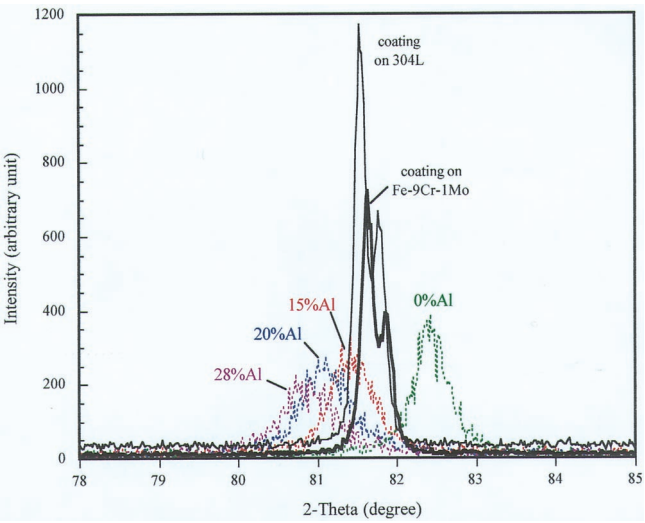


**Figure 5** X-ray diffraction results for cast alloys and coatings on Fe-9Cr-1Mo and 304L. At this location, there are two peaks for the coating and a single peak for the cast alloys which shifts with Al content.

Results for the coating on 304L appear to show a slightly higher Al content as the peak shift is greater than for the coating on Fe-9Cr-1Mo. However, this could also be attributed to an effect of Ni in the coating, which is not present in the other substrate. It is possible that the location and shape of this peak may be a non-destructive means of evaluating the Al content in the coating.

## CHARACTERIZATION OF COATED 304L

Initial exposures at 800°C in air, air + 10vol.%$H_2O$ and $H_2S$-$H_2O$-$H_2$-Ar showed promising mass change results for the CVD coatings [10]. Characterization of the reaction products has been completed that further elucidates the coating benefit. Figure 6 shows metallographic polished cross-sections on 304L with and without the coating and the effect of water vapor after a 24 h exposure at 800°C. Figures 6a and 6b show the thin reaction product formed in air with and without the CVD coating, respectively. At 800°C, 304L would not require a coating for service in air. However, when 10%$H_2O$ was added to the environment, the reaction product was significantly thicker without a coating, Figure 6c. The coated specimen showed no significant change with the addition of water vapor, Figure 6d. This same specimen also was characterized using EPMA, Figure 7. Figure 7a is a back-scattered electron image similar to the light microscopy image in Figure 6d. X-ray maps of O, Ni and Al are shown in Figures 7b–7d. The O map shows a continuous surface oxide with little oxygen penetration into the coating, Figure 7b. The Ni and Al maps show Ni-Al precipitates in the coating and an enrichment of both elements near the coatings surface. Figure 8 shows a composition profile in the coating after the 24h, 800°C exposure in air + 10%$H_2O$. Compared to the as-deposited composition, Figure 4, the Ni and Al contents in the outer coating layer actually appear higher with less Al in the inner layer. This change could be associated with a preference for intermetallic phase formation but these differences also may be a location dependence effect or due to a coating to coating variation. More work is necessary to confirm this change in composition with exposure. However, it does appear clear from these results that, with an aluminide coating, 304L is much more resistant to environments containing water vapor.

## CHARACTERIZATION OF COATED FE-9CR-1MO

Figure 9 shows metallographically polished cross-sections on Fe-9Cr-1Mo with and without the coating and the effect of water vapor on the amount of reaction after 24 h at 800°C. As was the case of 304L, dry air oxidation at 800°C resulted in a thin, protective reaction layer on uncoated Fe-9Cr-1Mo, Figure 9a. A similar thin oxide was formed on the coated substrate, Figure 9b. Uncoated Fe-9Cr-1Mo also was adversely affected by the addition of 10%$H_2O$, Figure 9c. The reaction layer appears thinner than that observed on 304L, Figure 6c. However, the cross-section did not include one of the large FeO nodules which formed on the specimen during this test. With the

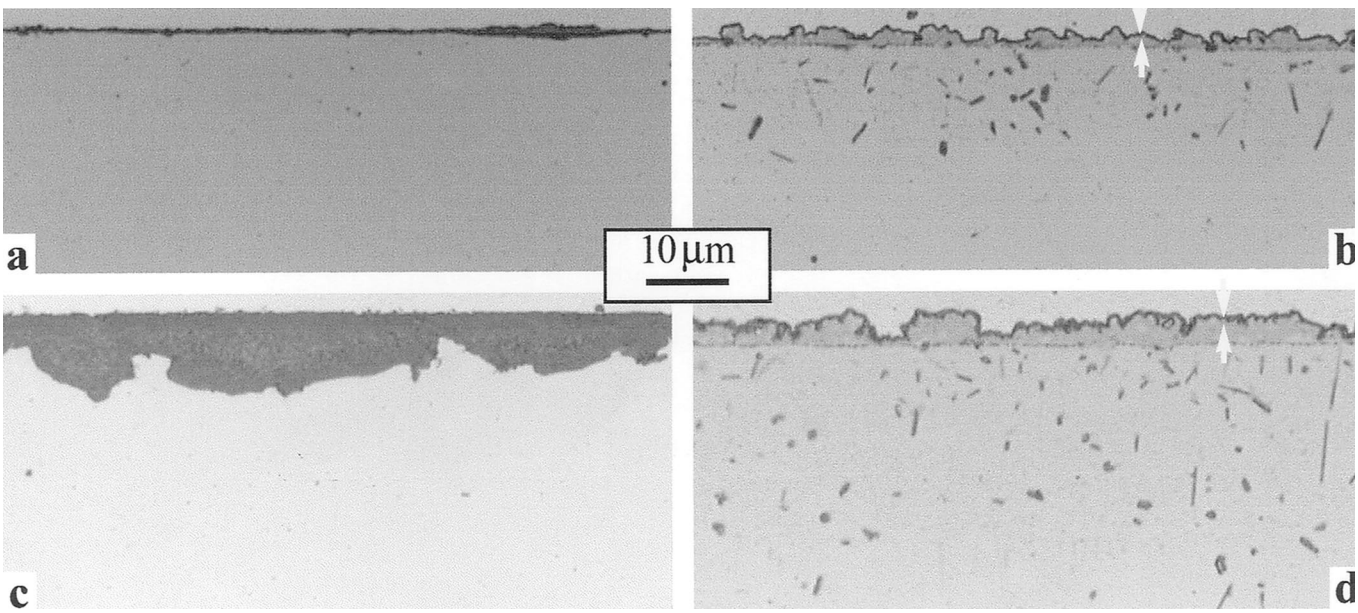


**Figure 6** Light microscopy images of cross-sections of 304L after 24 h at 800°C uncoated in (a) air and (c) air+10%$H^2O$ and with an aluminide coating in (b) air and (d) air+10%$H_2O$. Without a coating, 304L was strongly attacked by water vapor. Arrows point to the thin oxide layer in (b) and (d).

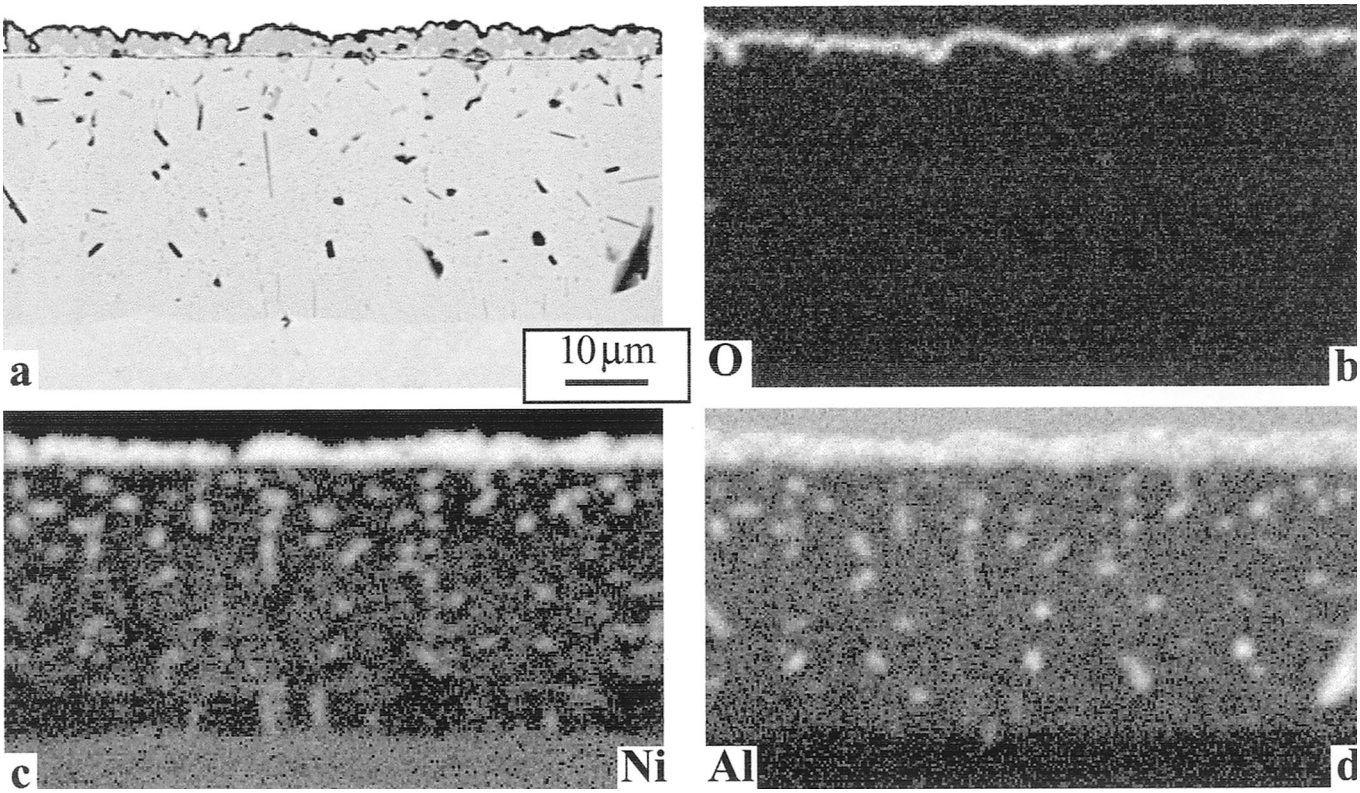


**Figure 7** (a) EPMA back-scattered electron cross-sectional electron image of coated 304L after 24 h at 800°C in air+10%$H_2O$. X-ray maps of the same region showing (b) O, (c) Ni and (d) Al. Oxygen was only detected in the surface oxide and not within the coating.

CVD coating, no accelerated attack was observed with the addition of water vapor. The coated specimen exposed for 24 h to air + 10%$H_2O$ also was examined by EPMA. Figure 10 shows a back-scattered electron image and the corresponding O, Cr and Al x-ray maps from the same area. The Al and O maps show a continuous $Al_2O_3$ external oxide and no oxygen penetration into the coating or substrate. There are a few Cr-rich precipitates in the coating and in the substrate, Figure 10c. The acicular particles concentrated near the substrate-coating interface are rich in Al, Figure 10d. Figure 11 shows a concentration profile through the exposed coating shown in Figure 10. The Al content in the coating has decreased to less than 10at.% except at the surface. The two peaks in the Al profile correspond to the Al-rich precipitates shown in Figure 10d. More particles appeared to form during the 24h, 800°C exposure and, like the coating on 304L, this coating showed a tendency toward intermetallic ($Fe_3Al$) phase formation. While the coating performed well in this test, the low Al content observed after completion suggests that the coating lifetime may be limited when made using these conditions.

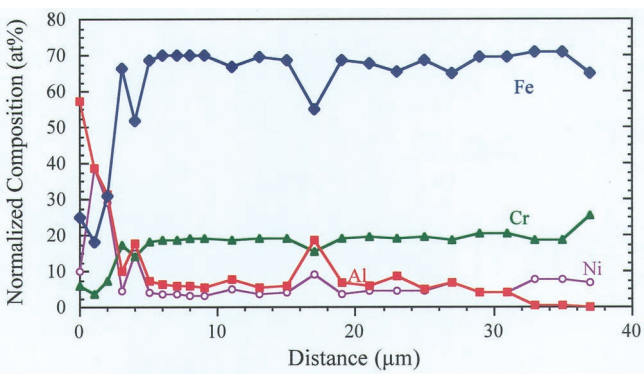


**Figure 8** Fe, Al Cr and Ni profiles in the coating on 304L after 24 h at 800°C in air+10%$H_2O$ using EPMA.

## CYCLIC OXIDATION AND SULFIDATION RESULTS

Based on the positive results observed in 24 h isothermal tests [10], cyclic experiments were conducted on similar coatings at 800°C. There are two purposes to a cyclic test. First, upon cooling after a cycle, any damage to the external alumina scale must be repaired in order to maintain the benefit during additional cycles. The coating must contain sufficient Al to reform the surface oxide or accelerated attack may occur. Second, any problem due to the CTE mismatch between the coating and substrate are exacerbated during thermal cycling.

Figure 12 shows results for 1h cycles conducted in air + 10%$H_2O$. Besides the coated and uncoated 304L and Fe-9Cr-1Mo specimens, several other compositions also were included. Figure 12a shows the benefit of coating both materials. For uncoated Fe-9Cr-1Mo, a high mass gain results from $FeO_x$ formation. This type of rapid attack would not be anticipated in a dry air environment. In contrast, uncoated 304L showed high mass losses during a 200 cycle exposure. The thick oxide formed in the presence of water vapor (e.g. Figure 6c) apparently continued to spall as a result of the thermal cycling.

Figure 12b shows results for the same test but with a smaller mass change range than Figure 12a that shows the benefit of the aluminide coatings on these materials. Small mass gains were noted for the coated substrates with little or no spallation noted for the coated Fe-9Cr-1Mo specimen. The mass gain was slightly higher for 304L and this specimen appeared to show some spallation

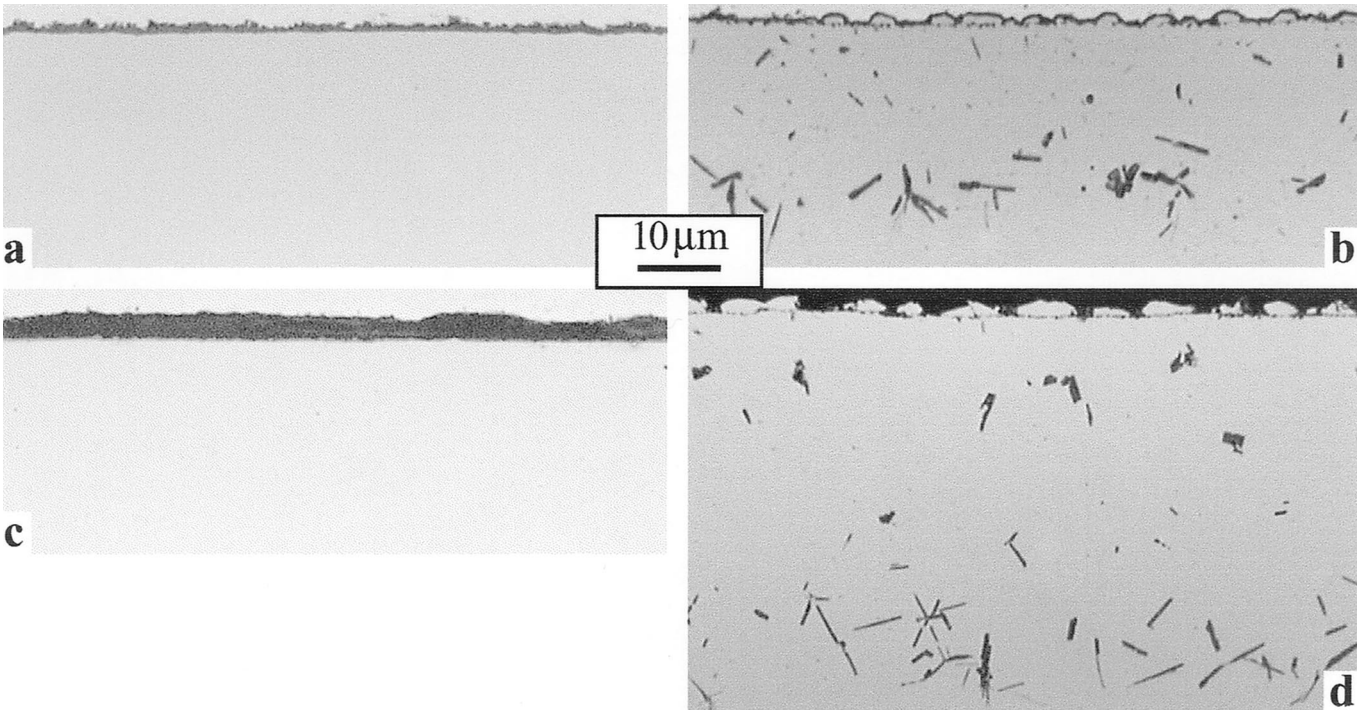


**Figure 9** Light microscopy images of cross-sections of uncoated Fe-9Cr-1Mo after 24 h at 800°C in (a) air and (c) air+10%$H_2O$ and with an aluminide coating in (b) air and (d) air+10%$H_2O$ Without a coating, Fe-9Cr-1Mo showed a much thicker oxide when exposed to water vapor.

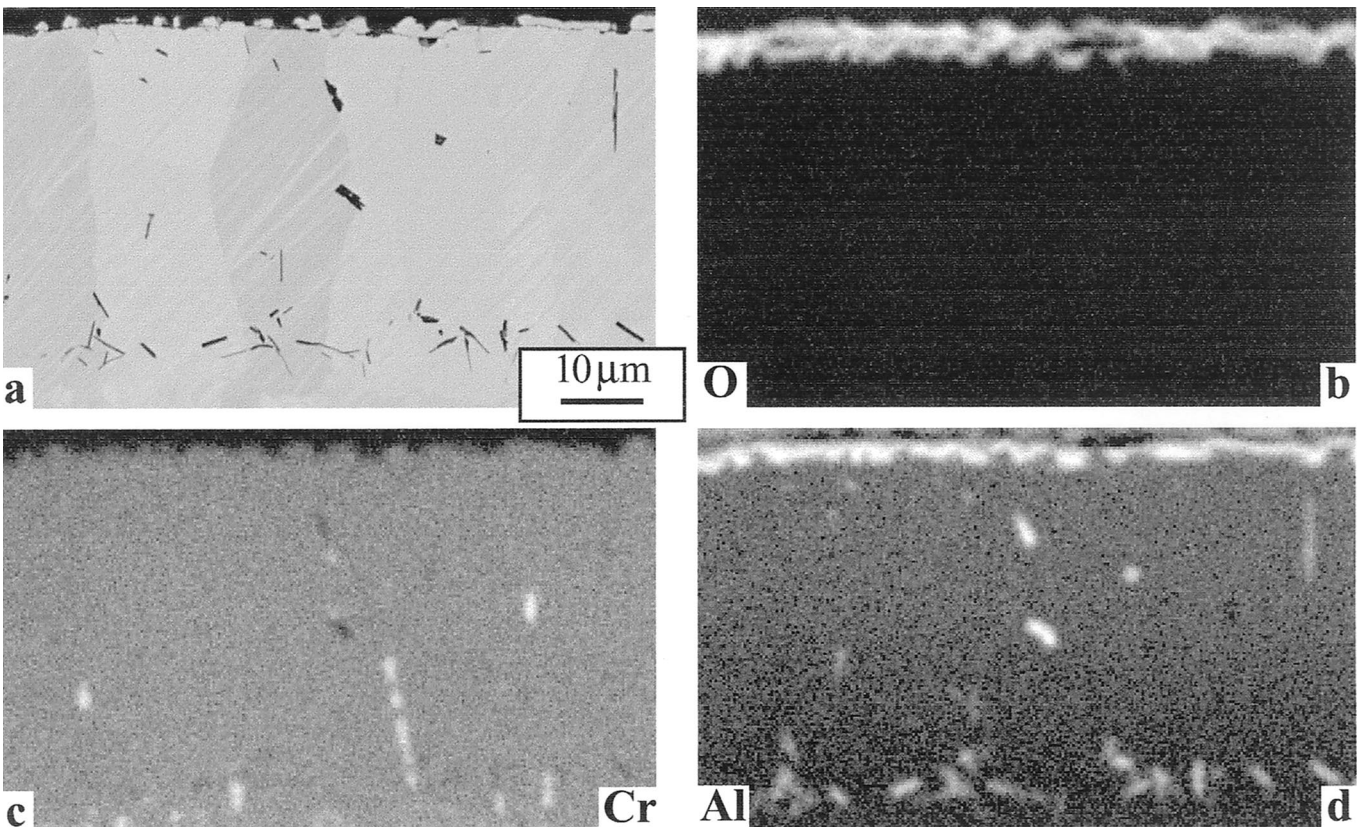


**Figure 10** (a) EPMA back-scattered electron cross-sectional electron image of coated Fe-9Cr-1Mo after 24 h at 800°C in air+10%$H_2O$. X-ray maps of the same region showing (b) O, (c) Ni and (d) Al. Oxygen was only detected in the surface oxide and not within the coating.

at the specimen edges. These specimens have not yet been characterized by metallography or SEM.

For comparison, a Fe-12Cr with VN (manufactured by ABB Alstrom) showed good oxidation resistance in this environment for 150 cycles but then was heavily attacked, likely due to Cr depletion. This improvement in behavior is expected in alloys with higher Cr contents, and better performance of the higher Cr content alloys was noted, Figure 12b. Specimens of NF709 (Fe-20Cr-25Ni) and Fe-18Cr-2Mo showed low mass changes during this test due to their higher Cr contents. The slight mass loss for NF709 is associated with the evaporation of $Cr(OH)_x$. Similar

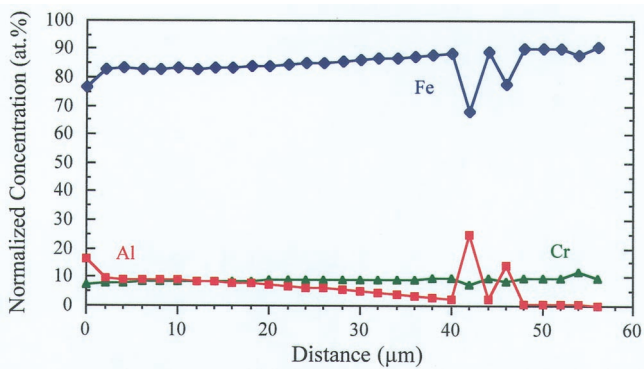


**Figure 11** Fe, Al and Cr profiles in the coating on Fe-9Cr-1Mo after 24 h at 800°C in air+10%$H_2O$ using EPMA.

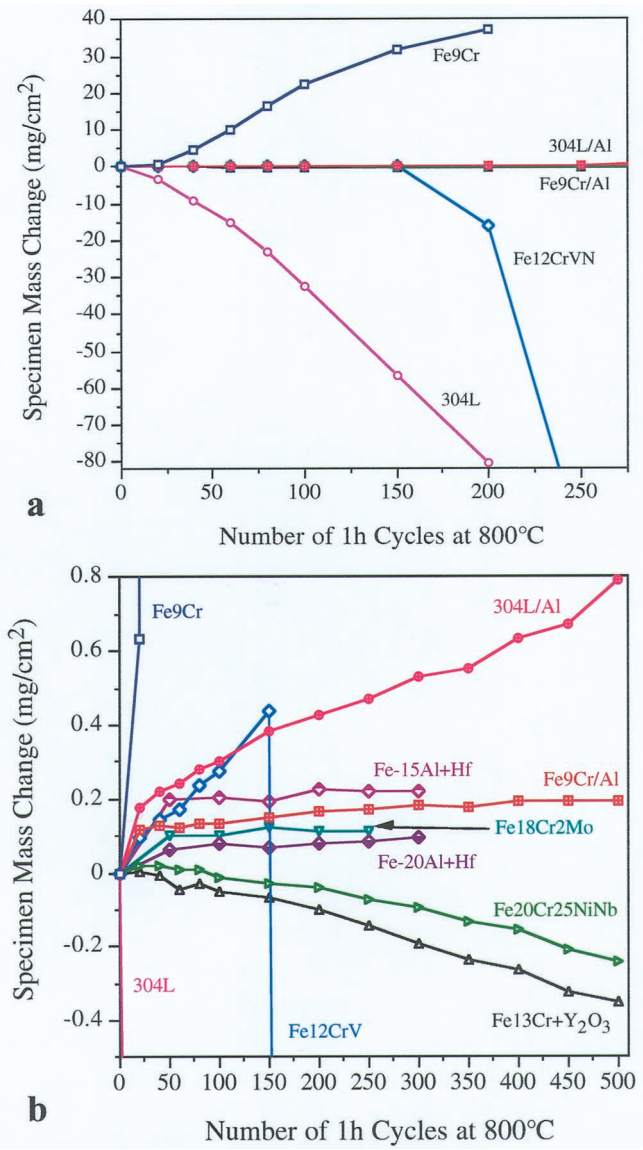


**Figure 12** Specimen mass changes during 1 h cycles at 800°C in air+10%$H_2O$.

performance was noted for an oxide dispersion strengthened (ODS) Fe-13Cr-3W specimen. In this case, the excellent oxidation resistance is attributed to the fine subgrain structure of the ODS material which allows for rapid, short-circuit Cr diffusion in the substrate. The benefit of short-circuit diffusion has been observed for both chromia- and alumina-forming substrates [15-19].

Cyclic exposures also was performed in a sulfidizing $H_2S$-$H_2O$-$H_2$-Ar environment. In this case, the equipment was not automated and ≈20–25h cycles were used instead of 1h cycles. However, the mass gain was monitored continuously by a microbalance. In the case of Fe-9Cr-1Mo, the improved performance of the specimen with an aluminized coating was excellent during the first 24 h, Figure 13a. However, in subsequent cycles, the mass gain increased dramatically, Figure 13b. (No mass gain was measured during the 4th cycle due to an equipment problem.) By the end of the 5th cycle, the large mass gain represents almost 50% of the specimen thickness consumed. Thus the coating did not continue to provide protection in this system. The coating performance degraded even more rapidly for 304L, Figure 14. The first 24 h showed good performance, Figure 14a, but the second 24 h resulted in essentially complete consumption of the specimen, Figure 14b. The relatively poor performance for the coatings could be attributed to their

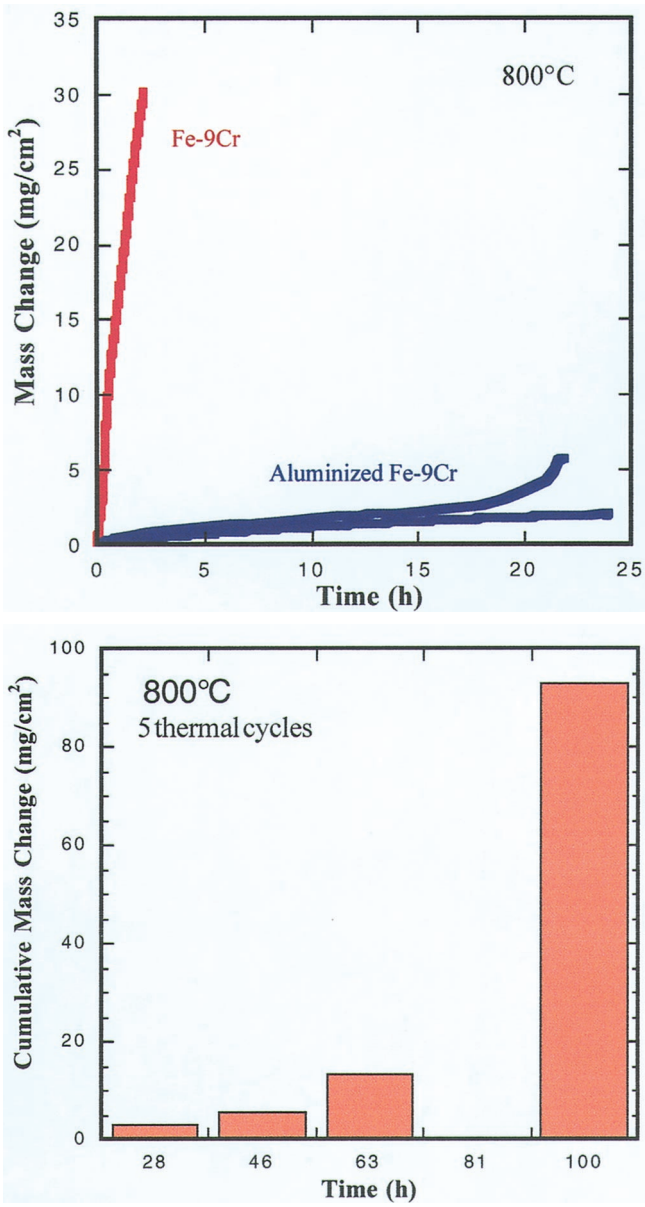


**Figure 13** For coating on Fe-9Cr-1Mo exposed to a sulfidizing environment at 800°C, (a) shows the mass gain during the first 24 h for two coated specimens compared to the uncoated material. In (b), the cumulative mass gain is shown for each of 5 cycles to a total of 100h. By the 5th cycle, the specimen was strongly attacked.

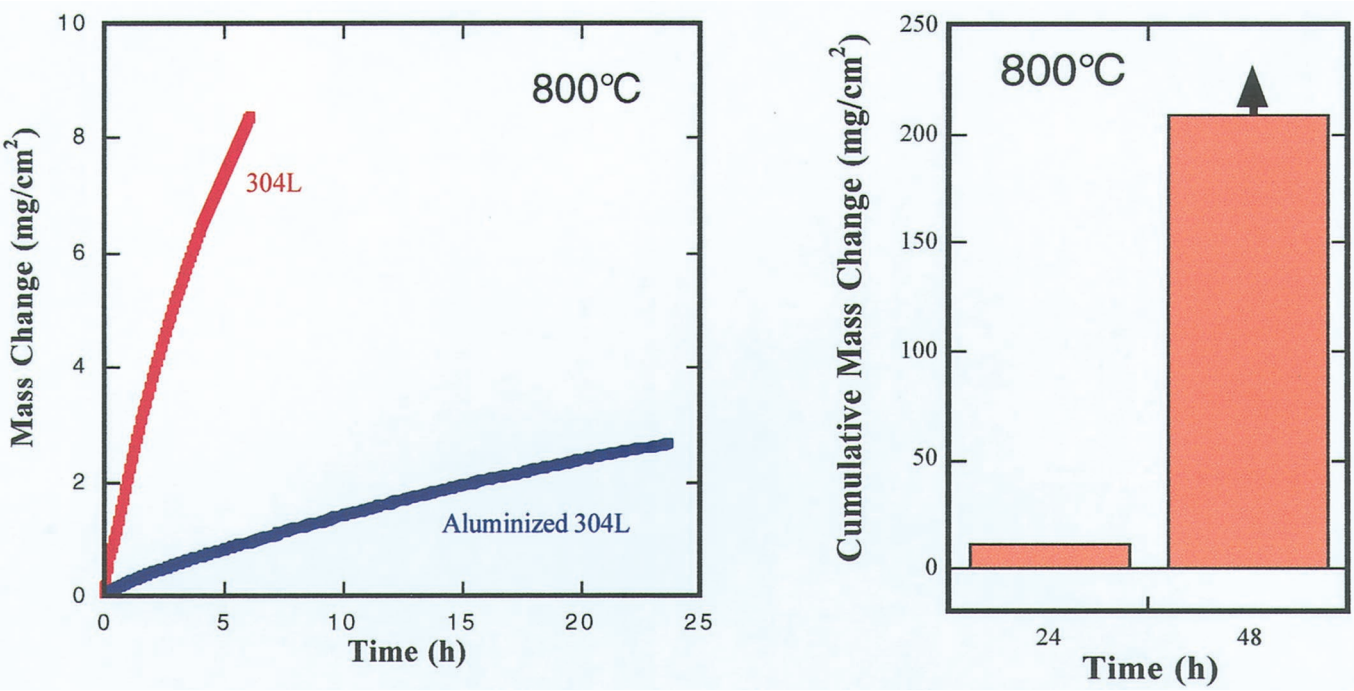


**Figure 14** For coating on 304L exposed to a sulfidizing environment at 800°C, (a) shows the mass gain during the first 24 h for a coated specimens compared to the uncoated material. In (b), the cumulative mass gain shows that after a second 24 h exposure, the specimen was completely consumed.

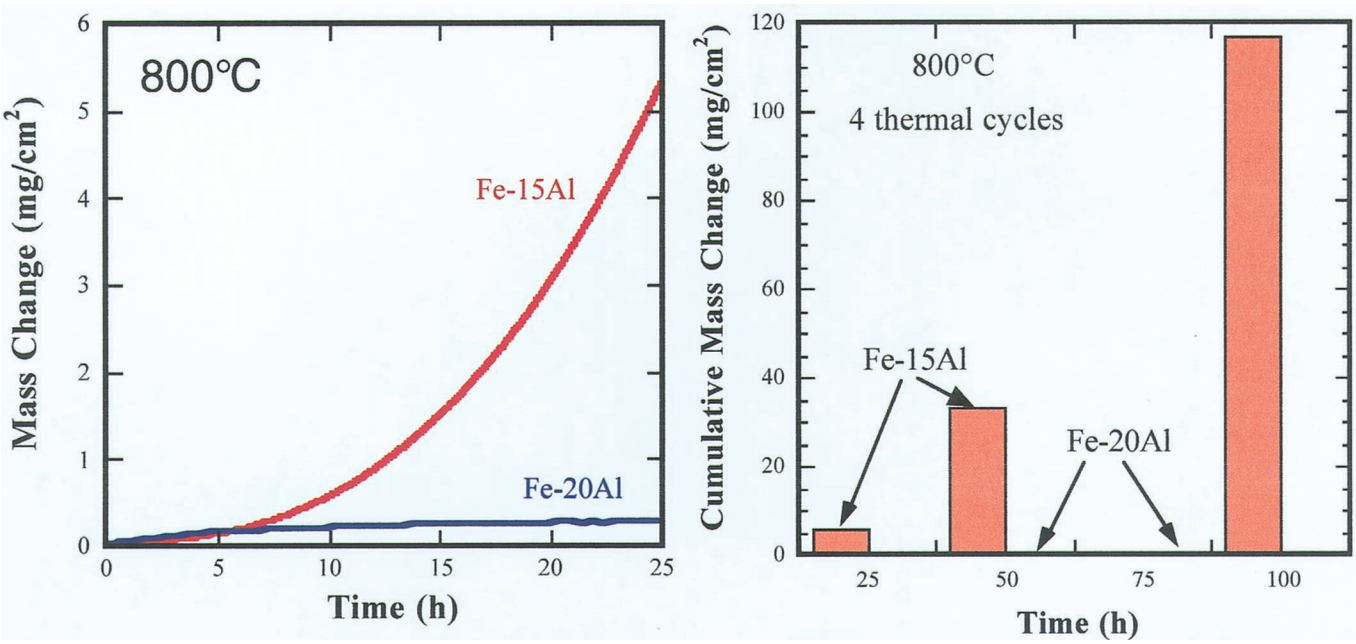


**Figure 15** For cast Fe-15Al and Fe-20Al exposed to a sulfidizing environment at 800°C, (a) shows the mass gain during the first 24 h and (b) shows the cumulative mass gain during subsequent cycles Increasing the Al content to 20at% resulted in a total mass change after 4 cycles of less than 0.2mg/cm$^2$.

low Al contents. Additional characterization of the coated specimens run for only 24 h is being performed to determine the Al contents and possibly provide more information on the cause of failure.

Previous work by DeVan and Tortorelli suggested that 18at.% Al was required for good sulfidation resistance of iron aluminides [4]. While the initial coating may contain that level of Al at the surface (Figures 2 and 4), after 24h at 800°C the Al contents were much lower on average (Figures 8 and 11). In addition, the enrichment of Ni in the outer layer of the coating on 304L may lead to the formation of $NiS_x$ which melts at <700°C. In order to explore the possible problems with low Al contents, cast alloys with 15 and 20at.%Al were exposed under the same conditions as the coatings. Figure 15a shows the higher mass gain observed for Fe-15Al compared to Fe-20Al. As with the coated substrates, Fe-15Al was fully consumed after 4 cycles totaling 101h at 800°C. As expected from the previous work [4], Fe-20Al showed much better sulfidation resistance in this test. Thermal cycling did not appear to affect the excellent performance during the first cycle, Figure 15a, and the total mass gain after 4 cycles was less than 0.2 mg/cm$^2$.

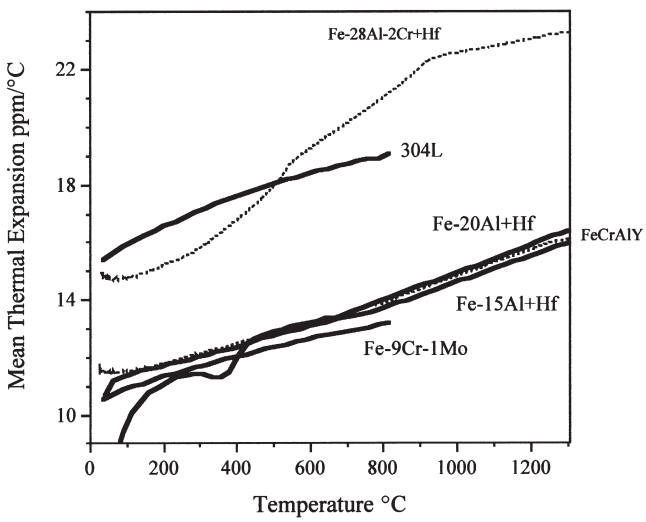


**Figure 16** Mean coefficient of thermal expansion as a function of temperature for various FeCrAl and Fe-Al substrates.

## CTE MEASUREMENTS

While the sulfidation tests show higher Al contents are desirable, previous work on $Fe_3Al$-type materials showed that their high CTE led to increased scale spallation compared to other Fe-base alloys [10–12]. This problem was first noted by Smialek and co-workers for Fe-40at.%Al [20]. While the CTE has been determined for FAL and FAS and ODS FAS, less information on CTE is available for lower Al contents. Therefore, Fe-15Al and Fe-20Al were examined to determine the effect of Al on the CTE of ferritic alloys. Figure 16 shows the CTE determined for these 2 cast materials along with that for FAS and FeCrAlY determined in a previous study and literature values for 304L and Fe-9Cr-1Mo [21–22]. These results indicate that the CTE for ferritic materials is essentially independent of Al content. By maintaining Al contents below $Fe_3Al$ (≈20at.%), good oxidation performance and a good CTE match with Fe-9Cr-1Mo could be achieved. However, since 304L has a higher CTE, it may be that a fully $DO_3$ structure may be more compatible. The higher CTE of 304L may be why the current coatings (with low Al and thus low CTE) did not perform as well in 1h cyclic testing as did the coating on Fe-9Cr-1Mo, Figure 12b. Future work will try to optimize coating composition and performance based on matching the substrate and coating CTE and sufficient Al to maintain corrosion resistance.

## SUMMARY

Coatings made by CVD aluminizing offer a potential method for synthesizing model corrosion-resistant coatings for oxidizing and sulfidizing environments. Present results show that CVD aluminized coatings have excellent resistance to environments containing water vapor but do not appear to have sufficient Al for long-term resistance to low oxygen, high sulfur environments. The different CTE of ferritic and austenitic substrates suggest different strategies for the optimum Al content in each case. The high CTE of 304L may be more compatible with $Fe_3Al$ coatings while the ferritic substrates should avoid the intermetallic phase formation.

## ACKNOWLEDGMENTS

The authors would like to thank K. Cooley, S. Waters, M. Howell, G. Garner and L. D. Chitwood at ORNL for assistance with the experimental work and J. R. DiStefano and C. G. McKamey at ORNL for their comments on the manuscript. This research was sponsored by the U.S. Department of Energy, Fossil Energy Advanced Materials Research Program under contract DE-AC05-00OR22725 with UT-Battelle, LLC.

## REFERENCES

[1] G. C. Wood, I. G. Wright, T. Hodgkiess, D. P. Whittle, "A Comparison of the Oxidation of Fe-Cr, Ni-Cr and Co-Cr Alloys in Oxygen and Water Vapor," Werk. Korr., 21 (1970) 900–10.

[2] B. A. Pint and J. M. Rakowski, "Effect of Water Vapor on the Oxidation Resistance of Stainless Steels," NACE Paper 00–259, Houston, TX, presented at NACE Corrosion 2000, Orlando, FL, March 2000.

[3] P. F. Tortorelli and J. H. DeVan, "Behavior of Iron Aluminides in Oxidizing and Oxidizing/ Sulfidizing Environments," *Mat. Sci. and Eng*., A153 (1992) 573–7.

[4] J. H. DeVan and P. F. Tortorelli, "The Oxidation-Sulfidation Behavior of Iron Alloys Containing 16–40at.% Aluminum," *Corr. Sci*., 35 (1993) 1065–71.

[5] K. Natesan and R. N. Johnson, "Corrosion Performance of Fe-Cr-Al and Fe Aluminide Alloys in Complex Gas Environments," in *Heat Resistant Materials II*, K Natesan, P. Ganesan and G. Lai, Eds., ASM Int.,Materials Park, OH, 1996, pp.591–9.

[6] P. F. Tortorelli and K. Natesan, *Mater. Sci. and Eng.* A258 (1998) 115.

[7] B. A. Pint, P. F. Tortorelli and I .G. Wright, "Long-Term Oxidation Performance of Ingot-Produced Fe3Al Alloys," *Mater. High Temp*., 16 (1999) 1–13.

[8] B. Jönsson and C. Svedberg, "Limiting Factors for Fe-Cr-Al and NiCr in Controlled Industrial Atmospheres," *Mater. Sci. Forum*, 251–4 (1997) 551–8.

[9] E. J. Opila and N. S. Jacobson, "Volatile Hydroxide Species of Common Protective Oxides and Their Role in High Temperature Corrosion," in *Fundamental Aspects of High Temperature Corrosio*n, D. A. Shores, R. A. Rapp, and P. Y. Hou, Eds., Proc. Vol.96–26, Electrochemical Society, Pennington, NJ, 1996, pp.344–56.

[10] B. A. Pint, P. F. Tortorelli, I. G. Wright, J. A. Haynes, and W. Y. Lee, "Evaluation Of Iron-Aluminide Coatings For High-Temperature Corrosion Protection," paper 1.X in Proc. Fourteenth Annual Conf. Fossil Energy Materials, R. R. Judkins (comp.), U. S. Department of Energy, 2000.

[11] I. G. Wright, B. A. Pint and P. F. Tortorelli, "The High Temperature Oxidation Behavior of ODS Fe3Al," *Oxid. Met*., 55 (2001) 333–57.

[12] B. A. Pint, K. L. More, P. F. Tortorelli, W. D. Porter and I. G. Wright, "Optimizing the Imperfect Oxidation Performance of Iron Aluminides," Mater. Sci. Forum, in press.

[13] G.V. Samsonov, *Oxide Handbook*, IFI/Plenum, New York, 1973.

[14] N. V. Bangaru and R. C. Krutenat, "Diffusion Coatings of Steels: Formation Mechanism and Microstructure of Aluminized Heat-Resistant Stainless Steels," *J. Vac. Sci. Technol. B*, 2 (1984) 806–15.

[15] D. R. Baer and M. D. Merz, "Differences in Oxides on Large- and Small-Grained 304 Stainless Steel," *Met. Trans*., 11A, 1973–80 (1980).

[16] G. J. Yurek, D. Eisen and A. Garratt-Reed, "Oxidation Behavior of a Fine-Grained Rapidly Solidified 18-8 Stainless Steel," *Met. Trans*., 13A, 473–85 (1982).

[17] M. J. Maloney and G. J. Yurek, "Improvements in Oxidation Resistance Through Rapid Solidification Processing," in *Composites/Corrosion-Coatings of Advanced Materials*, Proc. Vol. IMAM-4, S. Kimura, A. Kobayashi, S. Umekawa, K. Nii, Y. Saito and M. Yoshimura, Eds., Materials Research Society, Pittsburgh, PA, 1989, pp.383–8.

[18] J. G. Goedjen and D. A. Shores, "The Effect of Alloy Grain Size on the Transient Oxidation Behavior of an Alumina-Forming Alloy," *Oxid. Met*., 37, 125–42 (1992).

[19] B. A. Pint, J. Leibowitz and J. H. DeVan, "The Effect of an Oxide Dispersion on the Critical Al Content in Fe-Al Alloys," *Oxid. Met*., 51 (1999) 183–99.

[20] J. L. Smialek, J. Doychak and D. J. Gaydosh, "Oxidation Behavior of FeAl + Hf, Zr ,B," *Oxid. Met*., 34 (1990) 259–75.

[21] ASME Boiler and Pressure Vessel Code: An International Code, The American Society of Mechanical Engineers, New York, NY, 1998.

[22] R. W. Swindeman, "A Review of Thermal/Mechanical Fatigue in Composite Tube Materials," unpublished research, ORNL, Oak Ridge, TN, 1996.